Environ Monit Assess (2022) 194:727
https://doi.org/10.1007/s10661-022-10415-y

Monitoring and assessment of *Dracaena*-based constructed vertical flow wetlands treating textile dye wastewater

Monali Muduli · Meena Choudhary · Soumya Haldar · Sanak Ray

Received: 26 February 2022 / Accepted: 30 August 2022 / Published online: 5 September 2022

Abstract The monitoring and assessment of multiple constructed vertical flow wetlands (CVFWs) treating textile dye wastewater (metanil yellow as dye) are studied covering three seasons. Three CVFWs (CVFW-1, dye—5 mg/l; CVFW-2, dye—50 mg/l; and CVFW-3, dye—100 mg/l) and a control (dye—5 mg/l) were used. The CVFWs with *Dracaena* (an ornamental plant) efficiently removed contaminants like dye, COD, NH_4^+-N, and PO_4^{3-}-P from the wastewater under varying inlet dye concentrations, indicating its dependence on meteorological conditions. Substantial dye removal was observed to be maximum in summer (control, 44.3%; CVFW-1, 75.1%; CVFW-2, 76.1%; CVFW-3, 46%), but lesser in winter (control, 45%; CVFW-1, 73.1%; CVFW-2, 76.8%; CVFW-3, 42.6%) and minimum in monsoon (control, 40.8%; CVFW-1, 63.5%; CVFW-2, 51.6%; CVFW-3, 37.1%), respectively. Efficiency was less in CVFW-3 as it observed plant stress due to higher inlet dye concentration. COD removal was higher in winter, followed by summer and monsoon. A first-order kinetic model was used to investigate the efficiency of the CVFW system w.r.t. contaminant removal. Various functional groups were characterized using Fourier transform infrared spectroscopy (FTIR) from the inlet and outlet water samples of different CVFWs. The *Dracaena* accumulated various elements and oxides during the treatment with no stress on its health. No effects on plant health highlight the suitability of *Dracaena* for textile wastewater treatment. The results were validated using statistical tools like the Mann–Whitney *U* test and principal component analysis (PCA).

Keywords Metanil yellow removal · Chemical oxygen demand · Kinetics · Principal component analysis · Fourier transform infrared · X-ray fluorescence

Supplementary Information The online version contains supplementary material available at https://doi.org/10.1007/s10661-022-10415-y.

M. Muduli · M. Choudhary · S. Haldar · S. Ray (✉)
Analytical and Environmental Science Division & Centralized Instrument Facility, CSIR-Central Salt & Marine Chemicals Research Institute, G.B. Marg, Bhavnagar 364002, India
e-mail: sanakray@csmcri.res.in

M. Muduli · M. Choudhary · S. Haldar · S. Ray
Academy of Scientific and Innovative Research (AcSIR), Ghaziabad 201002, India

Introduction

Annually approximately 70 million tonnes of synthetic dyes is generated each year globally, primarily utilized in the manufacturing of textiles, cosmetics, and leather. About 30 to 150 thousand tonnes of dye-containing wastewater is released into the water bodies (Zou & Wang, 2017). Nowadays, the world is fascinated by using various synthetic dyes, and azo dye is famous for its applications. Nearly 70% of dyes were used as a coloring material in multiple industries, categorized under the azo group (Benkhaya et al., 2020). Azo dyes are substances that contain one or more azo linkages and are made up of a diazotized amine coupled to an amine or a phenol. Aromatic amines are the primary precursors of azo colors (Chung, 2016). In the past, at least 3000 azo dyes were used in the paper and pharmaceutical sectors, printing inks, paints, varnish, lacquer, and wood stains. Azo dyes are also used as colorants in synthetic and natural textile fibers, hair dyes, waxes, petroleum, plastics, and leather (Chung, 2016). The azo compounds have antibacterial, antiviral, antifungal, and cytotoxic properties in addition to their typical coloring activity (Ali et al., 2018). The azo double-bound groups are harmful and difficult to degrade in nature, potentially leading to significant environmental concerns and harming public health. Therefore, azo dye effluent must be treated before being released into aquatic bodies (Li et al., 2016).

Metanil yellow as an azo dye is used in various sectors, viz., food, pharmaceutical, leather, paper, textile, and chemical laboratories. Metanil yellow (a non-permitted food color) has been used as a food additive in making sweets, spices, pulses, beverages, and soft drinks to enhance their appearance (Kourani et al., 2020). Consumption of metanil yellow for a more extended period stimulates oxidative stress, prevents the indigenous antioxidant system, and produces free radicals. Moreover, it has a toxic impact on the digestive, excretory, reproductive, cardiovascular, and nervous systems, respectively (Ghosh et al., 2017). The presence of the azo group in metanil yellow blocks the sunlight in the aquatic environment, which affects the photosynthetic organisms and their activity (Ramadhani et al., 2020). The byproduct of the azo group, i.e., aromatic amine, causes various disorders like allergic, mastitis, skin irritation, gene alteration, etc. (Yaseen & Scholz, 2017). Although many researchers have developed methods like coagulation, chemical precipitation, electro-Fenton, electrochemical oxidation, and other advanced oxidation processes (Matyszczak et al., 2020) for the effective treatment of synthetic dye wastewater, all corresponding concern high operational and maintenance cost, vast applications of chemicals and electrical energy are the shortcomings of these methods.

Constructed wetlands (CWs) are considered sustainable and cost-effective approaches that undergo both phytoremediation and microbial remediation while treating various wastewaters (Muduli et al., 2022). The use of CWs for dye removal and textile wastewater is under investigation. Multiple researchers have reviewed the effectiveness of CWs in treating textile wastewater and dye removal (Dogdu & Yalcuk, 2016; Haddaji et al., 2019; Oon et al., 2020); however, very scanty literature is available covering all seasons. Under anaerobic conditions, the azo bond (present in the azo dye) can be broken easily to undergo the decolorization process; further, primary amine as a product can be degraded under aerobic conditions (Tee et al., 2015). Therefore, combining aerobic and anaerobic processes is advisable for complete dye degradation. Treatment of the metanil yellow dye using water hyacinth and specific bacterial strains like *Bacillus* sp. AK1 and *Lysinibacillus* sp. AK2 has been studied (Anjaneya et al., 2011; Guerrero-Coronilla et al., 2019).

Literature related to metanil yellow (acid yellow 36) removal using CWs is inadequate; furthermore, the use of ornamental species in the constructed vertical flow wetlands (CVFWs) is the uniqueness of this study. *Dracaena reflexa* is an ornamental species that has been used in the present study instead of wetland species. The main aim for choosing *Dracaena reflexa* is to undergo phytoremediation of textile wastewater, as it can withstand various environmental conditions and is simple to propagate by stem cuttings. Moreover, the root system of *Dracaena* has a propensity to develop micro-aerobic regions, contributing to the continuous degradation of organic matter (Dadrasnia & Pariatamby, 2016). In addition, the availability of native wetland species, especially in the arid and semi-arid areas, is challenging, where ornamental plants can play a vital role in wastewater management.

The present study uses CVFWs, which provide proper aeration (Hussein & Scholz, 2018) for the dye removal. This work aims to monitor and assess the *Dracaena*-based CVFWs' potentiality for treating synthetic wastewater contaminated with metanil yellow, chemical oxygen demand (COD), and nutrients like NH_4^+-N and PO_4^{3-}-P, respectively. The related objective was to (i) monitor the treatment efficiency (dye and other physicochemical contaminants) of the CVFWs operated in different seasons, (ii) kinetics of dye and nutrients removal, (iii) statistical analysis to validate pollutant removal, (iv) characterize the compounds present in the inlet and outlet water samples using Fourier transform infrared (FTIR), (v) elemental and oxide accumulation study of *Dracaena* by using X-ray fluorescence (XRF), (vi) compare the efficiency of the systems concerning the different concentration of dye mixture, and (vii) study the impact of synthetic dye mixture on the plant development.

Material and methods

Lab-scale CVFW setup, design, and operation

The experimental setups were made from opaque PVC pipes (to prevent algae growth) with a 4-inch diameter and 24-inch height (for providing space for grow of the plant root), providing an empty volume of 4.94 l. Each system was filled with two different natural media in layers with a particle size of 25–35 mm (gravels) and 8–12 mm (pea gravels) from bottom to up to support the plant species. CVFWs like CVFW-1, CVFW-2, and CVFW-3 were planted with the ornamental plant species named *Dracaena reflexa* except control system to study the influence of plant species on the treatment efficiency. The whole experimental setup was shown (Fig. 1). After plantation (single plant in each CVFW), the CVFWs were kept for 2 months to stabilize. The daily inlet dye mixture (synthetic wastewater) was 24 h for different CVFWs. This batch-scale experimental setup was located (21.7590° N, 72.1443° E) within the Council of Scientific and Industrial Research-Central Salt And Marine Chemicals Research Institute (CSIR-CSMCRI) Bhavnagar district of Gujarat. The system is exposed to ambient meteorological conditions. The CVFWs undergo vertical down-flow movement of wastewater. The outlet samples were collected every day (10 AM, with 24-h interval) from the outlet valve present at the bottom of each CVFW and were analyzed based on three seasons (summer, 02.03.2020 to 14.07.2020; monsoon, 17.07.2020 to 30.09.2020; and winter, 27.10.2020 to 24.11.2020), and the sample collection was stopped from 25 March to 7 June 2020 due to nationwide lockdown imposed by the Government of India for COVID-19 pandemic.

Characteristics of wastewater

Metanil yellow (acid yellow 36) is a commercial azo dye used in this study. The stock solution (1000 ppm) of the dye was prepared. The required concentrations for our investigation, i.e., 5 ppm, 50 ppm, and 100 ppm of volume 2 l, were prepared from the stock solution. In each dye concentration

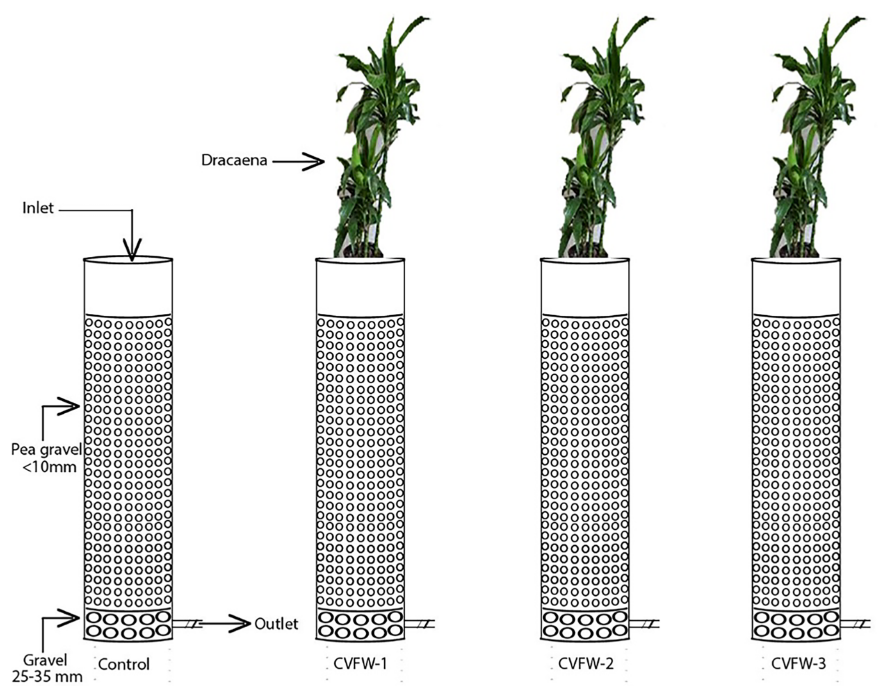

Fig. 1 Schematic diagram of the experimental setup treating the textile dye wastewater

(i.e., 5, 50, 100 ppm), an equal amount of nutrients, i.e., diammonium hydrogen phosphate and potassium nitrate, were added. The dye mixtures were prepared inside the laboratory at a temperature of about 25 °C by mixing all compounds properly (Table 1). During this study, all the used chemicals were analytical grade.

Water quality analysis

Inlet and outlet samples were sampled and analyzed correctly. Parameters like pH and TDS were measured on the spot immediately after sampling, and the remaining parameters (COD, color removal, chlorophyll estimation, nitrate, phosphate, and ammonium) were analyzed as per the procedure prescribed (APHA, 2017; Mohanty et al., 2015; Ray et al., 2014a). BOD analysis for water samples was not conducted as COD typically oxidizes more organic compounds chemically rather than biologically (Lee et al., 2016).

Chemical contaminants from water

The inlet and outlet water samples were analyzed using FTIR (Perkin Elmer, Model: Spectrum GX) (Ladwani, 2016) to see the presence of functional groups.

Biochemical characterization of *Dracaena*

Roots and stem from each CVFW were collected and analyzed during summer and winter for different biochemical characteristics. For ash content, the oven-dried roots and stem samples were kept in the muffle furnace at 500 °C for 30 min. Further, the ash was dissolved in distilled water, and the filtrate was analyzed to determine the nutrient uptake (nitrogen, phosphorous). The chlorophyll concentrations (chlorophyll-a, chlorophyll-b, and total chlorophyll) were undertaken for leaf samples, where the leaf was collected under dark conditions and was analyzed.

Table 1 Wastewater composition

Wetland type	Metanil yellow (mg/l)	$(NH_4)_2HPO_4$ (mg/l)	KNO_3 (mg/l)	Wastewater volume (l)
Control	5	14	12.48	2
CFW-1	5	14	12.48	2
CFW-2	50	14	12.48	2
CFW-3	100	14	12.48	2

*Metanil yellow: color index name—acid yellow 36, molecular composition—$C_{18}H_{14}N_3NaO_3S$, molecular weight (g/mol)—375.38, λmax (nm)—439, chemical class—mono azo (anionic), solubility—water; daily average inflow volume—2 l; daily average outflow volume—1.9 l

Elemental analysis

The dried pulverized forms of plants (roots and stem) and media (composite sample: both gravels and pea gravel) samples were pressed to form homogeneous pellets using boric powder as a binder and further analyzed using "wavelength dispersive X-ray fluorescence spectrometer" (WDXRF, Model: Bruker S8 TIGER II) delivers with its high sense technology for all elements from "Be to Am." Elemental compositions of the samples were analyzed by "complete analysis vac 34 mm" methods (Muduli et al., 2022).

Kinetic study

First-order kinetics model (Gajewska et al., 2020) was used to study the removal rate of the pollutants (COD, NH_4^+-N, and PO_4^{3-}-P) and dye through the systems. Microsoft Excel-2010 was used for the evaluation of decomposition rate.

Statistical analysis

The statistical analysis was undertaken using Statistical Package for Social Sciences (SPSS) (Ver 22) (Ray et al., 2014b, 2019). Mann–Whitney *U* test was used to elucidate whether any significant difference exists between seasons concerning parameters. The principal component analysis (PCA) was undertaken to explain the inter-relationship between different parameters. The mean and standard deviation was calculated using Microsoft Office Excel 2010. The experimental data were collected in triplicates, and the mean was considered for interpretation with an experimental error within ± 5%.

Results and discussion

Meteorological observations

Meteorological data like ambient air temperature, rainfall, and humidity were recorded (India Meteorological Department, 2020) and analyzed during the study, as they significantly influence the efficiency of the CWs during wastewater treatment (Yin et al., 2017). The ambient air temperature varied from 22.95 to 32.7 °C during the study, representing the local steppe climate. The average (±SD) ambient air temperatures for summer, winter, and monsoon were 28.7±2.6, 29.7±0.7, and 25.6±1.9 °C, respectively. The rainfall was observed only in monsoon and varied from 0 to 1.4 mm, whereas the average (±SD) humidity for summer, monsoon, and winter were 69.9±12.9, 78.7±6.8, and 36±5.4%, respectively.

Performance of the CVFWs for pollutant removal

During wastewater treatment, removing pollutants like dye, COD, PO_4^{3-}-P, and NH_4^+-N is a primary concern (Hussein & Scholz, 2018). During the study, the concentrations of the above pollutants were measured for both inlet and outlet water samples (Table 2). Over the study period, the inlet water quality showed not much variation for all the CVFWs (control, CVFW-1, CVFW-2, and CVFW-3) as they were prepared in the laboratory. In contrast, outlet water showed variation, especially for all the CVFWs planted with *Dracaena*, highlighting its role and dependence on meteorological factors.

Substantial dye removal was observed during the study period, maximum in summer, slightly lesser in winter, and the least in monsoon, respectively (Table 2). The dye removal in CVFW-3 is less than in CVFW-2, which may be due to the stress of a more significant inlet concentration of dye on *Dracaena.* Dye removal was achieved due to phytoremediation activities and media adsorption. Here the CVFWs with *Dracaena* can efficiently remove dye (37.1–76.8%) as compared with the previous study reported, i.e., 18–92%, treating other dyes (BR46, AB113, and mixture of BR46 and AB113) using common reed (a wetland plant species) (Hussein & Scholz, 2018). The relationship between ambient air temperature, air humidity, and dye removal during the study period is shown in Fig. 2. During summer, dye removal coincides with temperature due to the increased metabolism of plants and microbes in the wetland system. However, in monsoon, high air humidity hampers the dye removal efficiency. In winter, less humidity accelerated the dye removal. Seasonal variation of COD, dye, NH_4^+-N, and PO_4^{3-}-P concentrations in different CVFWs were shown (Figs. 3 and 4).

The inlet COD variation may be due to changing dye concentrations for different CVFWs; however, substantial COD removal was observed during the study period, maximum in winter, slightly lesser in summer, and the least in monsoon, respectively (Table 2). The COD removal in CVFW-3 is less than in CVFW-2, which may be due to the stress of a more significant dye concentration on *Dracaena*. The COD removal was observed in CVFWs with the *Dracaena* plant highlighting its phytoremediation characteristics. Here the CVFWs with *Dracaena* can efficiently remove COD (50.5–72.3%) as compared with the previous study reported (Hussein & Scholz, 2018), i.e., 37–82%, treating other dyes using common reed. The relationship between ambient air temperature, air humidity, and COD removal during the study period is shown in Fig. 2. During summer, COD removal coincides with temperature, which may be due to the increased metabolism of plants and microbes in the wetland system; however, high air humidity hampers COD removal efficiency in monsoon. An increase in temperature would lead to a rise in carbon and nitrogen removal and vice versa. In winter, decreasing humidity accelerated the dye removal.

In this study, CVFWs could efficiently remove nutrients like PO_4^{3-}-P (19.5–58.2%) and NH_4^+-N (93.1–96.7%) (Table 2). In summer, the PO_4^{3-}-P removal efficiency was more than the other two seasons; the reason may be the higher rate of evapotranspiration and nutrient uptake (Nandakumar et al., 2019). Media adsorption and chemical precipitation may be the other reason for PO_4-P reduction. Here gravels (low in cost and collected locally) worked as reactive media as it contains Al, Ca, and Fe having a better affinity for phosphorus (Yin et al., 2017). The composite sample was collected at the end of the experiment and the elemental composition for gravels (control—Al: 48,900 ppm, Ca: 127,000 ppm, Fe: 78,400 ppm; CVFW-1—Al: 49,700 ppm, Ca: 142,000 ppm, Fe: 75,300 ppm; CVFW-2—Al: 43,800 ppm, Ca: 124,000 ppm, Fe: 74,900 ppm; CVFW-3—Al: 40,700 ppm, Ca: 115,000 ppm, Fe: 74,700 ppm) was analyzed using WDXRF. Better

Table 2 Performance of the *Dracaena*-based constructed vertical flow wetland (CVFW) system during different seasons

Seasons	Wetland types	Parameters	Observations	Inlet			Outlet			Removal (%)
				Min	Max	Mean ± SD	Min	Max	Mean ± SD	
Summer	Control	Dye (mg/l)	34	5	5.95	5.5 ± 0.2	0.55	5.3	3 ± 0.9	44.3
		COD (mg/l)	34	28	36	32.4 ± 2.2	28	36	32 ± 2.1	0.9
		TDS (mg/l)	9	483	517	505.6 ± 1	483	552	532 ± 56	n/a
		PO_4^{3-}-P (mg/l)	7	2.92	3.26	3.1 ± 0.1	1.69	1.89	1.7 ± 0.1	43
		NH_4^+-N (mg/l)	7	2.99	3.45	3.2 ± 0.1	0.06	0.16	0.1 ± 0	96.5
		DO (mg/l)	7	8.18	8.64	8.3 ± 0.1	2.72	3.77	3 ± 0.4	n/a
		pH	9	7.92	8.23	8 ± 0.1	7.61	8.2	7.8 ± 0.1	n/a
	CVFW-1	Dye (mg/l)	34	5	5.95	5.5 ± 0.2	0.1	2.2	1.3 ± 0.4	75.1
		COD (mg/l)	34	28	36	32.4 ± 2.2	8	16	12.3 ± 2.1	61.8
		TDS (mg/l)	9	483	517	505.6 ± 17	544	664	581 ± 36.3	n/a
		PO_4^{3-}-P (mg/l)	7	2.92	3.26	3.1 ± 0.1	1.18	1.48	1.3 ± 0.1	58.2
		NH_4^+-N (mg/l)	7	2.99	3.45	3.2 ± 0.1	0.05	0.19	0.1 ± 0	96.5
		DO (mg/l)	7	8.18	8.64	8.3 ± 0.1	2.77	3.77	3.3 ± 0.4	n/a
		pH	9	7.92	8.23	8 ± 0.1	7.26	7.73	7.5 ± 0.1	n/a
	CVFW-2	Dye (mg/l)	34	50	59.25	52.2 ± 2.4	8	18.55	12.4 ± 2.8	76.1
		COD (mg/l)	34	62	72	68.2 ± 3.2	12	26	20.1 ± 4.1	70.5
		TDS (mg/l)	9	507	550	535.6 ± 21.5	621	728	666.6 ± 34.7	n/a
		PO_4^{3-}-P (mg/l)	7	2.92	3.26	3.1 ± 0.1	1.22	1.49	1.3 ± 0.1	57.2
		NH_4^+-N (mg/l)	7	2.99	3.45	3.2 ± 0.1	0.03	0.14	0.1 ± 0	96.7
		DO (mg/l)	7	8.15	8.64	8.3 ± 0.1	2.58	3.5	3.1 ± 0.3	n/a
		pH	9	8.08	8.21	8.1 ± 0	7.29	7.7	7.5 ± 0.1	n/a
	CVFW-3	Dye (mg/l)	34	100	115.15	107 ± 4.3	37.45	69.8	57.6 ± 6.7	46
		COD (mg/l)	34	96	130	113.1 ± 9.9	30	66	45.9 ± 11.5	59.4
		TDS (mg/l)	9	550	584	572.6 ± 17	637	782	712.4 ± 44.5	n/a
		PO_4^{3-}-P (mg/l)	7	2.92	3.26	3.1 ± 0.1	1.26	1.5	1.3 ± 0.1	56.3
		NH_4^+-N (mg/l)	7	2.99	3.45	3.2 ± 0.1	0.1	0.32	0.1 ± 0.1	94.4
		DO (mg/l)	7	8.15	8.64	8.4 ± 0.1	2.58	3.5	3.1 ± 0.3	n/a
		pH	9	8.06	8.29	8.1 ± 0.1	7.29	7.72	7.5 ± 0.1	n/a
Monsoon	Control	Dye (mg/l)	19	5.22	5.61	5.4 ± 0.1	2.66	3.7	3.2 ± 0.2	40.8
		COD (mg/l)	19	28	34	32 ± 1.6	28	34	32 ± 1.6	Nil
		TDS (mg/l)	9	483	517	505.6 ± 17	483	552	532.5 ± 22.8	n/a
		PO_4^{3-}-P (mg/l)	19	2.92	3.26	3.1 ± 0.1	2.25	2.65	2.5 ± 0.1	19.5
		DO (mg/l)	19	8.15	8.64	8.3 ± 0.1	2.42	3.52	3 ± 0.4	n/a
		pH	34	7.8	8.23	8 ± 0.1	7.61	8.2	7.8 ± 0.2	n/a
	CVFW-1	Dye (mg/l)	19	5.22	5.61	5.4 ± 0.1	1.05	3.13	2 ± 0.7	63.5
		COD (mg/l)	19	28	34	32 ± 1.6	12	18	15.7 ± 1.6	50.5
		TDS (mg/l)	9	483	517	505.6 ± 17	544	664	581 ± 36.3	n/a

Table 2 (continued)

Seasons	Wetland types	Parameters	Observations	Inlet			Outlet			Removal (%)
				Min	Max	Mean ± SD	Min	Max	Mean ± SD	
		PO_4^{3-}-P (mg/l)	19	2.92	3.26	3.1 ± 0.1	1.67	1.87	1.8 ± 0.1	42.3
		DO (mg/l)	19	8.15	8.64	8.3 ± 0.1	2.58	3.77	3.1 ± 0.3	n/a
		pH	34	7.8	8.23	8 ± 0.1	7.62	8.35	8 ± 0.1	n/a
	CVFW-2	Dye (mg/l)	19	50	51.61	50.6 ± 0.7	12.27	30.87	24.4 ± 4.4	51.6
		COD (mg/l)	19	62	72	68.3 ± 2.9	22	34	29.1 ± 4.6	57.2
		TDS (mg/l)	9	507	550	535.6 ± 21.5	621	720	666.1 ± 32.9	n/a
		PO_4^{3-}-P (mg/l)	19	2.92	3.26	3.1 ± 0.1	1.5	1.8	1.6 ± 0.1	48.3
		DO (mg/l)	19	8.15	8.64	8.4 ± 0.1	2.78	3.54	3.1 ± 0.2	n/a
		pH	34	8.06	8.45	8.1 ± 0.1	7.5	7.98	7.8 ± 0.1	n/a
	CVFW-3	Dye (mg/l)	19	100	105.22	101.4 ± 1.9	45.35	80.7	63.5 ± 12.3	37.1
		COD (mg/l)	19	102	130	113.7 ± 8	45	65	55.6 ± 6	51
		TDS (mg/l)	9	550	584	572.6 ± 17	637	782	711.4 ± 43.6	n/a
		PO_4^{3-}-P (mg/l)	19	2.92	3.26	3.12 ± 0.1	1.59	1.79	1.6 ± 0.1	46
		DO (mg/l)	19	8.13	8.64	8.4 ± 0.1	2.79	3.54	3.1 ± 0.2	n/a
		pH	34	8.15	8.5	8.2 ± 0.1	7.66	8.09	7.8 ± 0.1	n/a
Winter	Control	Dye (mg/l)	9	5.23	5.94	5.5 ± 0.2	2.23	3.85	3 ± 0.6	45
		COD (mg/l)	9	32	39	33.2 ± 2.3	32	38	32.8 ± 2	0.9
		TDS (mg/l)	9	432	475	451.4 ± 16.1	418	549	469.4 ± 36.6	n/a
		PO_4^{3-}-P (mg/l)	9	2.92	3.26	3.1 ± 0.1	1.76	1.96	1.8 ± 0.1	40.6
		NH_4^+-N (mg/l)	9	2.98	3.67	3.2 ± 0.2	0.02	0.74	0.2 ± 0.2	93.1
		NO_3^--N (mg/l)	9	1.7	1.9	1.7 ± 0.1	2.4	2.9	2.6 ± 0.1	n/a
		DO (mg/l)	9	8.15	8.6	8.4 ± 0.1	2.76	2.96	2.8 ± 0.1	n/a
		pH	9	7.9	8.23	8 ± 0.1	7.61	8.2	7.8 ± 0.2	n/a
	CVFW-1	Dye (mg/l)	9	5.23	5.94	5.5 ± 0.2	1.19	2	1.4 ± 0.2	73.1
		COD (mg/l)	9	32	39	33.2 ± 2.3	8	16	11.8 ± 2.5	64.4
		TDS (mg/l)	9	432	475	451.4 ± 16.1	430	495	467.3 ± 20.3	n/a
		PO_4^{3-}-P (mg/l)	9	2.92	3.26	3.1 ± 0.1	1.64	1.85	1.7 ± 0.1	43.7
		NH_4^+-N (mg/l)	9	2.98	3.67	3.2 ± 0.2	0.07	0.19	0.1 ± 0	96.2
		NO_3^--N (mg/l)	9	1.7	1.9	1.7 ± 0.1	3	3.3	3.1 ± 0.1	n/a
		DO (mg/l)	9	8.15	8.6	8.4 ± 0.1	2.73	3.46	2.9 ± 0.2	n/a
		pH	9	7.9	8.23	8 ± 0.1	7.39	7.94	7.6 ± 0.2	n/a
	CVFW-2	Dye (mg/l)	9	53.99	57.14	55.2 ± 0.9	8.8	14.23	12.8 ± 1.7	76.8
		COD (mg/l)	9	62	72	68.2 ± 3.5	12	24	18.8 ± 5.2	72.3
		TDS (mg/l)	9	313	488	447.8 ± 53.5	443	506	479.2 ± 19.9	n/a
		PO_4^{3-}-P (mg/l)	9	2.92	3.26	3.1 ± 0.1	1.36	1.62	1.4 ± 0.1	53.7

Table 2 (continued)

Seasons	Wetland types	Parameters	Observations	Inlet			Outlet			Removal (%)
				Min	Max	Mean ± SD	Min	Max	Mean ± SD	
		NH_4^+-N (mg/l)	9	2.98	3.67	3.2 ± 0.2	0.06	0.24	0.1 ± 0.4	95.6
		NO_3^--N (mg/l)	9	1.7	1.9	1.7 ± 0.1	2	2.2	2.1 ± 0.1	n/a
		DO (mg/l)	9	8.15	8.57	8.2 ± 0.1	2.58	3.47	3 ± 0.3	n/a
		pH	9	8.07	8.33	8.1 ± 0.1	7.11	8.15	7.5 ± 0.3	n/a
	CVFW-3	Dye (mg/l)	9	102.42	110.04	106.5 ± 2.9	52.38	67.19	60.9 ± 4.7	42.6
		COD (mg/l)	9	100	130	113 ± 9.4	30	60	42.5 ± 9.9	62.5
		TDS (mg/l)	9	451	492	472.5 ± 15	450	510	488.1 ± 22.5	n/a
		PO_4^{3-}-P (mg/l)	9	2.92	3.26	3.1 ± 0.1	1.56	1.75	1.6 ± 0.1	47.2
		NH_4^+-N (mg/l)	9	2.98	3.67	3.2 ± 0.2	0.01	0.25	0.1 ± 0.1	96.2
		NO_3^--N (mg/l)	9	1.7	1.9	1.7 ± 0.1	1.75	1.95	1.8 ± 0.1	n/a
		DO (mg/l)	9	8.15	8.64	8.4 ± 0.1	2.79	3.54	3.1 ± 0.3	n/a
		pH	9	8.06	8.39	8.2 ± 0.1	7.2	8.05	7.5 ± 0.3	n/a

Dye azo dye metanil yellow, acid yellow 36, *COD* chemical oxygen demand, *TDS* total dissolved solids, PO_4^{3-}*-P* phosphate phosphorous, NH_4^+*-N* ammonium nitrogen, NO_3^-*-N* nitrate nitrogen, *DO* dissolved oxygen, *SD* standard deviation, average air temperature, °C (summer: 28.7 ± 2.6SD, monsoon: 29.7 ± 0.7SD, winter: 25.6 ± 1.9SD), average air humidity, % (summer: 69.9 ± 12.9SD, monsoon: 78.7 ± 6.8SD, winter: 36 ± 5.4SD), average rainfall, mm (monsoon: 0.1 ± 0.3)

NH_4^+-N removal was achieved, which may be due to proper aeration enhancing the nitrification activities. The vertical hydraulic flow pattern and the rhizosphere zone of *Dracaena* enhanced the oxygen level. However, NO_3^--N concentration increased, which may be resulted from ammonia oxidation. The average TDS outlet concentration slightly exceeds the inlet (Table 2), observed in an earlier study (Hussein & Scholz, 2018). The average pH and DO values were given for both inlet and outlet water samples (Table 2). Overall the treatment performance of the wetland system was higher in both summer and winter, followed by the monsoon, where temperature and humidity play a vital role.

First-order kinetics model

The first-order kinetics model was used as a reliable tool to investigate the efficiency of a working system related to contaminant removal. Gajewska et al. (2020) have mentioned the first-order kinetics model for a vertical flow constructed wetland in their study.

$$\frac{C_{Out}}{C_{In}} = e^{\frac{-K_A}{q}} \tag{1}$$

By solving Eq. (1), we can get

$$K_A = -q \ln \frac{C_{Out}}{C_{In}} \tag{2}$$

where K_A: decomposition rate constant in m/d; C_{out}: outlet concentration in mg/l; C_{in}: inlet concentration in mg/l; and q: hydraulic loading rate in m d^{-1}.

Using Eq. (2), we calculated the decomposition rate constants for various parameters like COD, dye, PO_4^{3-}-P, and NH_4^+-N for different seasons. From Table 3, we found a remarkable removal rate, i.e., 0.33, was achieved by CVFW-1, especially in the summer season compared to the control system. However, both systems have been treated with the same concentration of dye mixture. This result indicated that plant species planted in CVFW-1 significantly contributed to the removal rate. From the decomposition rate constant value calculated for the other two systems named CVFW-2 and CVFW-3 treated with 50 and 100 ppm dye, respectively, we realized that CVFW-2 had greater K_A value, i.e., 0.34, during summer as compared to the other three systems. This result indicated that using *Dracaena*, we can treat dye mixture up to 50 ppm. Concentration more than 50 ppm may create a stressful condition for that plant species.

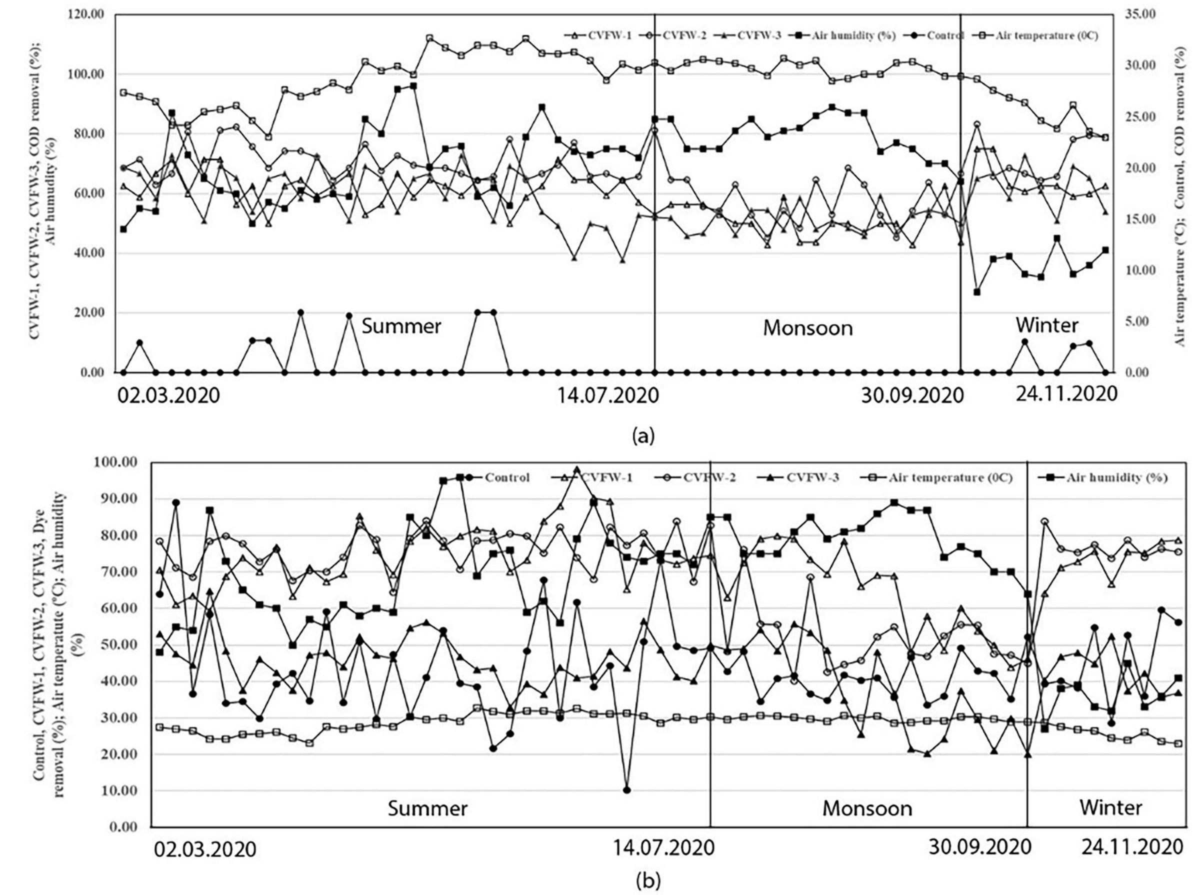

Fig. 2 Relationship of temperature (°C) and air humidity (%) with **a** COD removal (%), **b** dye removal (%)

Moreover, during summer, high ambient temperature provides a favorable condition to the plant species to treat the dye mixture.

By analyzing the K_A value of COD for four CVFWs, i.e., control, CVFW-1, CVFW-2, and CVFW-3, we observed a greater K_A, i.e., 0.308, by CVFW-2. From this result, we may conclude that the winter season may be providing favorable conditions to that plant species for the removal of COD. During the experiment, excellent performance was observed for removing NH_4^+-N by all systems. K_A value of NH_3-N varies between 0.6 and 0.9 for all CVFWs. Between two seasons, i.e., summer and monsoon, the out-standing K_A value of NH_3-N, i.e., 0.81, was achieved during summer. The design and configuration of all the systems and rhizospheric bacteria present around the root zones of plant species is the key contributor to the oxidation of NH_4^+-N. Decomposition rate constants for PO_4^{3-}-P of all seasons by all the four reactors were studied, and we got to know that K_A was found to be between 0.1 and 0.2. CVFW-3 achieved higher removal during summer. Both phyto-accumulation and adsorption by gravels used inside the CVFWs contributed towards PO_4^{3-}-P removal.

Statistical analysis

Mann–Whitney U test

In this study, the removal of various water pollutants during treatment using different CVFWs was considered to see whether seasonal variance has any impact on them or not using the "Mann–Whitney *U* test," and the variations are shown (Table 7, supplementary file). Significant ($p<0.05$) dye removal was observed for CVFW-1

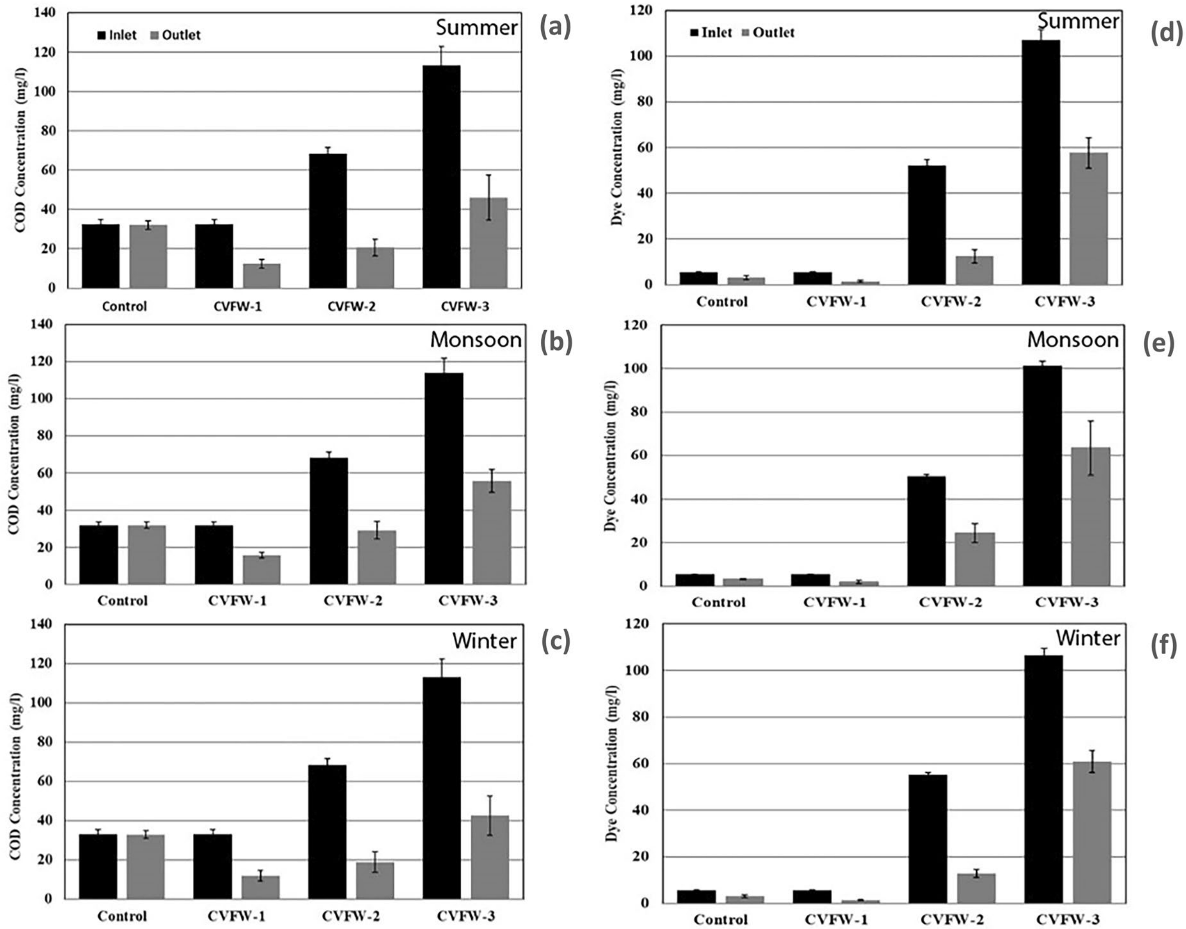

Fig. 3 Variation of COD and dye concentrations in different CVFWs **a** summer; **b** monsoon; **c** winter; **d** summer; **e** monsoon; **f** winter

(summer-monsoon) and CVFW-2 (summer-monsoon and monsoon-winter). Similarly significant COD removal was observed for control (summer-monsoon), CVFW-1 (summer-monsoon and monsoon-winter), CVFW-2 (summer-monsoon and monsoon-winter), and CVFW-3 (summer-monsoon and monsoon-winter). Significant differences were observed in the case of dye, COD, and PO_4^{3-}-P removal, highlighting the impact of seasonal variation, whereas NH_4^+-N removal is independent of meteorological factors.

Principal component analysis

The PCA used in the present study helped to concise the information collected to a lesser set of critical, independent variables (Fig. 5). It was used to establish the relationship within the experimental variables (air temperature, pH, air humidity, COD, dye, DO, NH_4^+-N, and PO_4^{3-}-P) during the treatment. All the above variables were described with three components. Component-1 describes 28.09 of the cumulative variance with an eigenvalue of 2.24. It comprises of variables like air temperature, pH, air humidity, and dye, showing a positive correlation and highlighting the dye removal dependency on meteorological factors. Similarly, component-2 describes 46.29 of the cumulative variance and eigenvalue of 1.45. Here it comprises variables like COD and dye, highlighting the COD value that includes dye. Component-3 contains DO, NH_4^+-N, and PO_4^{3-}-P, which shows the dependency of NH_4^+-N removal on DO and PO_4^{3-}-P uptake by *Dracaena* and media adsorption.

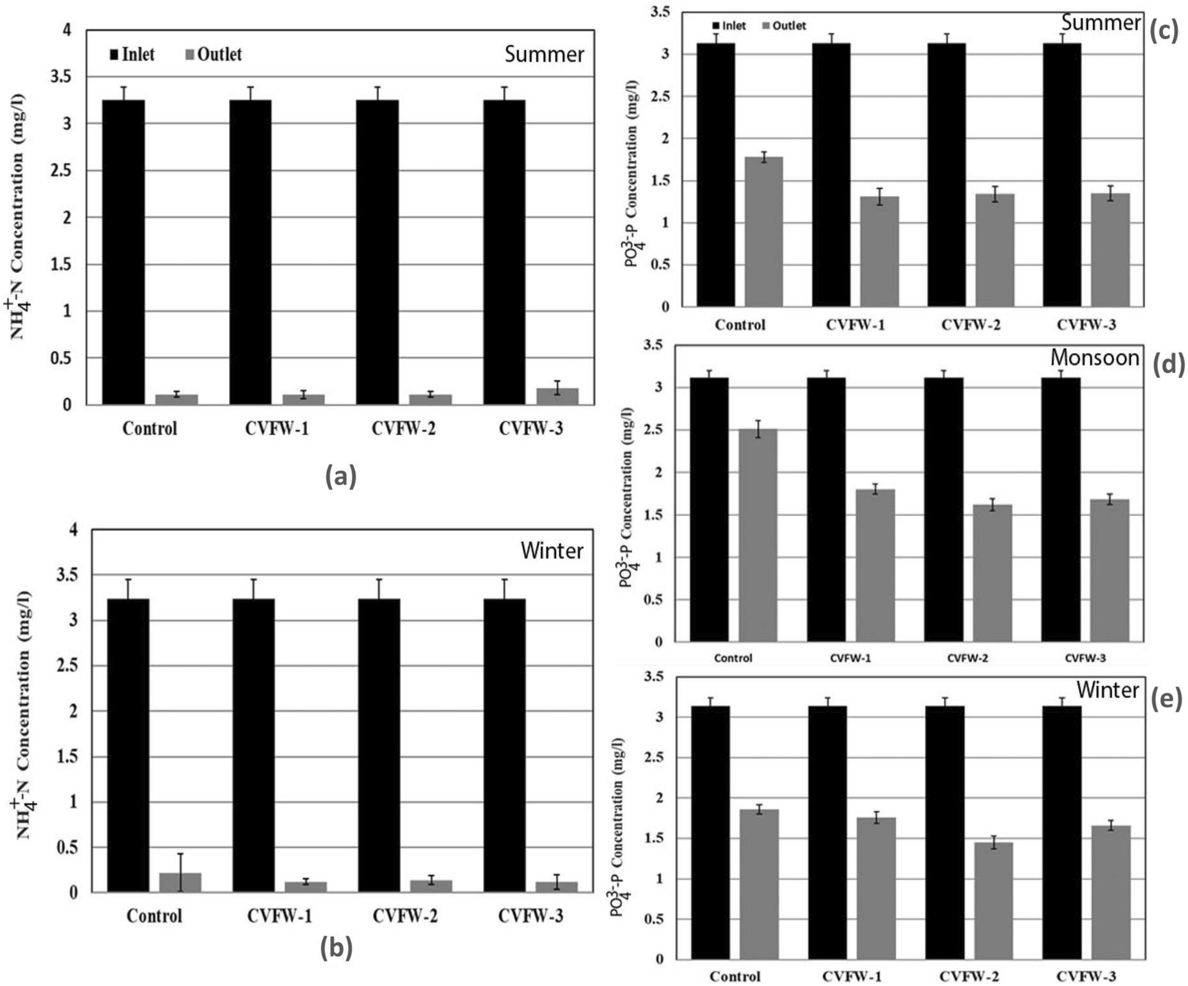

Fig. 4 Variation of NH_4^+-N and PO_4^{3-}-P concentrations in different CVFWs **a** summer; **b** winter; **c** summer; **d** monsoon; **e** winter

FTIR spectral analysis

By analyzing both inlet and outlet samples of different CVFWs, i.e., control, CVFW-1, CVFW-2, and CVFW-3, by FTIR, we observed the presence of various functional groups and their intensities (Table 4). The comparative study of inlet and outlet of the wastewater (dye mixture) of concentration 5 ppm treated by control and CVFW-1, as shown in Fig. 6 (supplementary file), stated a remarkable change in the intensity of the functional group. A great shifting in intensity was noticed for the peak azide (2160–2120 cm^{-1}) in CVFW-1 compared to control. This better result in CVFW-1 may be due to phyto-accumulation and media absorption. From FTIR peak at 3340.92 cm^{-1} of the outlet of control, i.e., N–H stretching, primary amine, we may predict that the formation of primary amine, a byproduct of the azo group, prevents further degradation process of dye.

By analyzing FTIR peaks of both inlet and outlet of CVFW-2, we observed no significant change in intensity of the azide group. But the peak at 1262.87 cm^{-1} (alkyl aryl ether, aromatic ester) found in the inlet was absent in the outlet and the peaks at 1159.89, 1087.48, 1017.86, 887.84, 819.03, 755.55, 687.62, and 621.97 cm^{-1} were found in the outlet. We may predict that the functional group alkyl aryl ether

Table 3 First-order kinetics

Seasons	Wetland types	Parameters	C_{in} (mg/l)	C_{out} (mg/l)	K_A (m/d)
Summer	Control	Dye	5.51	3.08	0.139
		COD	32.41	32.09	0.002
		PO_4^{3-}-P	3.13	1.78	0.135
		NH_4^+-N	3.25	0.11	0.813
	CVFW-1	Dye	5.51	1.37	0.334
		COD	32.41	12.38	0.231
		PO_4^{3-}-P	3.13	1.31	0.209
		NH_4^+-N	3.25	0.11	0.813
	CVFW-2	Dye	52.21	12.47	0.344
		COD	68.29	20.18	0.293
		PO_4^{3-}-P	3.13	1.34	0.204
		NH_4^+-N	3.25	0.11	0.813
	CVFW-3	Dye	107.06	57.65	0.148
		COD	113.12	45.97	0.216
		PO_4^{3-}-P	3.13	1.37	0.198
		NH_4^+-N	3.25	0.18	0.694
Monsoon	Control	Dye	5.48	3.24	0.13
		COD	32	32	0
		PO_4^{3-}-P	3.12	2.51	0.052
	CVFW-1	Dye	5.48	2.01	0.24
		COD	32	15.79	0.169
		PO_4^{3-}-P	3.12	1.8	0.132
	CVFW-2	Dye	50.66	24.45	0.175
		COD	68.32	29.16	0.204
		PO_4^{3-}-P	3.12	1.62	0.157
	CVFW-3	Dye	101.45	63.55	0.112
		COD	113.79	55.68	0.172
		PO_4^{3-}-P	3.12	1.68	0.148
Winter	Control	Dye	5.52	3.3	0.123
		COD	33.22	32.89	0.002
		PO_4^{3-}-P	3.14	1.86	0.125
		NH_4^+-N	3.24	0.22	0.645
	CVFW-1	Dye	5.52	1.48	0.315
		COD	33.22	11.89	0.246
		PO_4^{3-}-P	3.14	1.76	0.138
		NH_4^+-N	3.24	0.12	0.791
	CVFW-2	Dye	55.24	12.8	0.351
		COD	68.22	18.89	0.308
		PO_4^{3-}-P	3.14	1.45	0.185
		NH_4^+-N	3.24	0.14	0.754
	CVFW-3	Dye	106.59	60.97	0.134
		COD	113	42.56	0.234
		PO_4^{3-}-P	3.14	1.66	0.153
		NH_4^+-N	3.24	0.12	0.791

A area, i.e., 0.0081 m^2, C_{out} outlet concentration, mg/l, C_{in} inlet concentration, mg/l, *q* hydraulic loading rate, m/d, K_A decomposition constant, m/d, *Dye* azo dye metanil yellow, acid yellow 36, *COD* chemical oxygen demand, PO_4^{3-}-*P* phosphate phosphorous, NH_4^+-*N* ammonium nitrogen and aromatic ester has got transformation during treatment to produce the alcohol, alkenes, aliphatic ethers, and various fluoro compounds.

By investigating the FTIR peak of both inlet and outlet of CVFW-3, we may state that a slight shift in intensity for the azide group has occurred (Fig. 7, supplementary file). Besides it, peaks (1260.71, 1021.81, 867.02, 806.61, 751.51, 632.99 cm^{-1}) disappeared in the outlet.

Elemental and oxide accumulation by *Dracaena*

The potential of *Dracaena* concerning elemental and oxide accumulation during treatment was observed in the present study while treating 262 l of wastewater from summer to winter, where composite samples were considered for analysis of root and stem. Metallic elements, viz., Al, Ti, Cr, Mn, Fe, Co, Ni, Cu, Zn, Mo, Ru, Pd, V, and W, and non-metallic elements, viz., Na, Mg, Si, P, S, Cl, K, Ca, Br, and Sr, were detected from root and stem of CVFW-1, CVFW-2, and CVFW-3, respectively (Table 5). Metallic element accumulation was observed for Mn (root—48%, stem—75.1%), Co (root—100%, stem—100%), Cu (root—30.3%, stem—7.7%), and Mo (root—100%, stem—100%) in CVFW-1, respectively. Accumulation in roots was observed for Cr (61.6%) and Ni (31.3%), whereas Al (25.7%) accumulation was observed in the stem. Similarly, nonmetallic element accumulation was observed for Na (root—34.5%, stem—89.4%), Mg (root—32.3%, stem—50.4%), Si (root—8.6%, stem—4.7%), S (root—28.1%, stem—65.3%), and Br (root—41.7%, stem—100%) in CVFW-1, respectively. Accumulation in stem was observed for P (58.3%), Cl (69.2%), K (5%), and Ca (63.7%). CVFW-1 accumulated oxides in both roots (CaO, MgO, Na_2O, K_2O, P_2O_5, MnO, SO_3, V_2O_5, SrO, CuO, Cr_2O_3, NiO, MoO_3, and CoO) and stem (SiO_2, Al_2O_3, Fe_2O_3, CaO, MgO, Na_2O, TiO_2, P_2O_5, MnO, SO_3, V_2O_5, SrO, CuO, ZnO, MoO_3, CoO), respectively (Table 5). Similarly, the elements and oxides for CVFW-2 and CVFW-3 are shown in Table 4. Overall in CVFW-2, the accumulation was observed to be more than CVFW-1 and CVFW-3. Moreover, the element accumulation was observed to be maximum in the stem compared with roots for all the *Dracaena*-based wetlands. For oxides, accumulation was observed to be more in roots. The source of these elements and oxides may be largely from the media used in the wetlands, and some might be from the chemicals used to prepare the synthetic wastewater. The accumulation by *Dracaena* proves to be a potential plant species, which may be used in treating real textile dye wastewater (that contains both dye and other toxic elements).

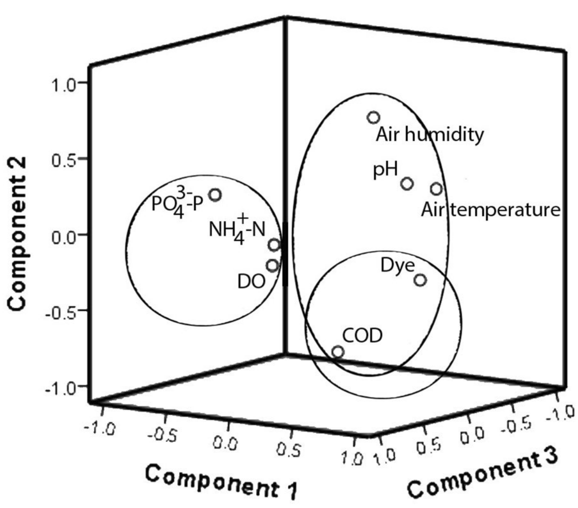

Fig. 5 Principal component analysis highlighting the relationship within the experimental variables (air temperature, pH, air humidity, COD, dye, DO, NH_4^+-N, and PO_4^{3-}-P) during the treatment

Wastewater effect on *Dracaena*

The biochemical components of plants were studied as they played a vital role in textile dye wastewater treatment and taking nutrients (nitrogen, phosphorous). The growth of the *Dracaena* plant was monitored in terms of ash content, chlorophyll (a, b, and total), and inorganic salts (nitrogen and phosphorous) within a gap of 9 months, from summer to winter (Table 6). A substantial increase in chlorophyll concentrations was observed for CVFW-1 and CVFW-2 with no physical stress on plant growth. In contrast, decreased chlorophyll in CVFW-3 shows plant stress imposed due to higher inlet dye concentration. The root ash content has increased for all CVFWs, whereas stem ash content is only observed to be decreased in CVFW-3.

Table 4 Infrared frequencies and identified functional groups from FTIR spectra

Wetland types	Inlet			Outlet		
	Frequency (cm^{-1})	Possibility of functional groups	Respective functional groups	Frequency (cm^{-1})	Possibility of functional groups	Respective functional groups
Control	3855.54	O–H stretching	Alcohol	3984.96	O–H stretching	Alcohol
	3391.42	O–H stretching	Alcohol	3340.92	N–H stretching	Aliphatic primary amine, secondary amine
	2127.93	N=N=N stretching	Azide	2132.71	N=N=N stretching, N=C=N stretching, CΞC stretching	Azide, carbodiimide, alkyne
	1871.37	C–H bending	Aromatic compound	1642.96	C=N stretching, C=C stretching	Imine/oxime, alkene, conjugated alkene
	1644.2	C=C stretching, N–H BENDING	Conjugated alkene, alkene, amine, cyclic alkene, alkene, imine/oxime	1262.93	C–O stretching	Aromatic ester, alkyl aryl ethers
	625.18	C–Br stretching	Halo compound	700.13	C=C bending	Alkene
	413.84			412.61		
CVFW-1	3372.66	O–H stretching, N–H stretching	Alcohol, aliphatic primary amine	3294.5	O–H stretching, C–H stretching	Carboxylic acid, alcohol, alkyne
	2127.53	N=N=N stretching, N=C=N stretching	Azide, carbodiimide	2131.79	CΞC stretching, N=C=N stretching, N=C=S stretching, N=N=N stretching, N=C=S stretching	Alkyne, carbodiimide, azide, isothiocyanate
	1643.87	C=C stretching, C=N stretching, C=C stretching	Conjugated alkene, imine/oxime, alkene	1642.98	C=N stretching, C=C stretching	Imine/oxime, alkene, conjugated alkene
	731.55	C–H bending	Mono substituted	700.8	C=C bending	Alkene
	412.48			413.33		

Table 4 (continued)

Wetland types	Inlet			Outlet		
	Frequency (cm^{-1})	Possibility of functional groups	Respective functional groups	Frequency (cm^{-1})	Possibility of functional groups	Respective functional groups
CVFW-2	3934.91	O–H stretching	Alcohol	3614.9	O–H stretching	Alcohol
	3467.72	O–H stretching	Alcohol	2127.13	N = N = N stretching, N = C = N stretching, CΞC stretching, N = C = S stretching	Azide, carbodiimide, alkyne, isothiocyanate
	3263.87	O–H stretching	Carboxylic acid	1651.18	C = N stretching, C = C stretching	Alkene, imine/oxime
	2131.49	N = N = N stretching, N = C = N stretching, CΞC stretching, N = C = S stretching	Azide, carbodiimide, alkyne, isothiocyanate	1159.89	O–H bending, C–F stretching, C–O stretching	Fluoro compound, tertiary alcohol
	1642.65	C = C stretching	Alkene, conjugated alkene	1087.48	C–O stretching,	Aliphatic ether, secondary alcohol
	1262.87	C–O stretching	Alkyl aryl ether, aromatic ester	1017.86		
	698.2	C–Br stretching	Halo compound	887.84	C = C bending	Alkene
	412.12			755.55	C–H bending	Mono substituted
				687.62	C–Br stretching	Halo compound
				621.62	C–Br stretching	Halo compound
				557.77	C–I stretching	Halo compound
				489.12		
				435.34		

Table 4 (continued)

Wetland types	Inlet			Outlet		
	Frequency (cm^{-1})	Possibility of functional groups	Respective functional groups	Frequency (cm^{-1})	Possibility of functional groups	Respective functional groups
CVFW-3	3928.44	O–H stretching	Alcohol	3937.15	O–H stretching	Alcohol
	3900.77	O–H stretching	Alcohol	3543.17	O–H stretching	Alcohol
	3647.53	O–H stretching	Alcohol	3262.99	O–H stretching	Alcohol, carboxylic acid
	3565.23	O–H stretching	Alcohol	2129.62	N = N = N stretching	Azide
	2126.5	N = N = N stretching, N = C = N stretching, CΞC stretching, N = C = S stretching	Azide, carbodiimide, Alkyne, isothiocyanate	1642.47	C = N stretching	Imine/oxime
	1651.86	C = N stretching, C = C stretching	Imine/oxime, alkene	701.25		Benzene derivative
	1260.71	C–O stretching	Aromatic ester, alkyl aryl ether	553.31		
	1021.81					
	867.02					
	806.61	C = C bending, C–Cl stretching	Alkene, halo compound			
	751.51	C–Cl stretching	Halo compound			
	632.99	C–Br stretching	Halo compound			
	474.93					

Table 5 Elemental and oxide accumulation by *Dracaena* in the wetlands during the study period

		Summer		Winter		Accumulation (%)	
				CVFW-1		CVFW-1	
		Root	Stem	Root	Stem	Root	Stem
Elements	Na (ppm)	1310	284	2000	2690	34.5	89.4
	Mg (ppm)	1130	1220	1670	2460	32.3	50.4
	Al (ppm)	408	1100	549	942	25.7	n/a
	Si (ppm)	1600	4070	1750	4270	8.6	4.7
	P (ppm)	1490	830	1180	1990	n/a	58.3
	S (ppm)	3090	1560	4300	4490	28.1	65.3
	Cl (ppm)	12,700	4470	11,700	14,500	n/a	69.2
	K (ppm)	27,400	6250	6750	6580	n/a	5.0
	Ca (ppm)	17,300	8640	14,600	23,800	n/a	63.7
	Ti (ppm)	194	489	n/d	300	n/a	n/a
	Cr (ppm)	96.7	116	252	n/d	61.6	n/a
	Mn (ppm)	156	96.7	300	389	48.0	75.1
	Fe (ppm)	3450	7820	2230	4230	n/a	n/a
	Co (ppm)	n/d	n/d	28.5	18.9	100.0	100.0
	Ni (ppm)	112	104	163	93.9	31.3	n/a
	Cu (ppm)	154	190	221	231	30.3	17.7
	Zn (ppm)	187	209	177	219	n/a	4.6
	Br (ppm)	186	n/d	319	414	41.7	100.0
	Sr (ppm)	725	331	598	111	n/a	n/a
	Mo (ppm)	n/d	n/d	385	423	100.0	100.0
	Ru (ppm)	420	583	421	524	0.2	n/a
	Pd (ppm)	n/d	459	n/d	915	n/a	49.8
	W (ppm)	n/d	n/d	n/d	829	n/a	100.0
	V (ppm)	n/d	n/d	n/d	127	n/a	100.0
Oxides	SiO_2 (ppm)	9100	3060	3790	9480	n/a	67.7
	Al_2O_3 (ppm)	2050	882	1220	1777	n/a	50.4
	Fe_2O_3 (ppm)	10,900	4820	3270	5730	n/a	15.9
	CaO (ppm)	12,400	24,100	20,200	33,300	38.6	27.6
	MgO (ppm)	2200	1910	2820	4230	22.0	54.8
	Na_2O (ppm)	387	1810	2850	3940	86.4	54.1
	TiO_2 (ppm)	758	413	184	527	n/a	21.6
	K_2O (ppm)	7400	33,100	8130	7760	9.0	n/a
	P_2O_5 (ppm)	1170	3270	2540	4480	53.9	27.0
	MnO (ppm)	162	163	360	488	55.0	66.6
	SO_3 (ppm)	3800	7550	10,800	10,700	64.8	29.4
	V_2O_5 (ppm)	99.8	n/d	150	244	33.5	100.0
	SrO (ppm)	379	851	766	1230	50.5	30.8
	CuO (ppm)	208	213	246	276	15.4	22.8
	Cr_2O_3 (ppm)	49.5	n/d	250	n/d	80.2	n/a
	ZnO (ppm)	287	218	220	284	n/a	23.2
	NiO (ppm)	88.6	125	189	n/d	53.1	n/a
	MoO_3 (ppm)	n/d	592	538	635	100.0	6.8
	CoO (ppm)	n/d	n/d	68.1	18.1	100.0	100.0

Table 5 (continued)

		Summer		Winter		Accumulation (%)	
				CVFW-2		CVFW-2	
		Root	Stem	Root	Stem	Root	Stem
Elements	Na (ppm)	1310	284	743	2690	n/a	89.4
	Mg (ppm)	1130	1220	1590	2460	28.9	50.4
	Al (ppm)	408	1100	2080	942	80.4	n/a
	Si (ppm)	1600	4070	4040	4270	60.4	4.7
	P (ppm)	1490	830	672	1990	n/a	58.3
	S (ppm)	3090	1560	9190	4490	66.4	65.3
	Cl (ppm)	12,700	4470	3930	14,500	n/a	69.2
	K (ppm)	27,400	6250	1810	6850	n/a	8.8
	Ca (ppm)	17,300	8640	16,500	23,800	n/a	63.7
	Ti (ppm)	194	489	997	300	80.5	n/a
	Cr (ppm)	96.7	116	179	n/d	46.0	n/a
	Mn (ppm)	156	96.7	687	389	77.3	75.1
	Fe (ppm)	3450	7820	17,000	4230	79.7	n/a
	Co (ppm)	n/d	n/d	n/d	18.9	n/a	100.0
	Ni (ppm)	112	104	232	93.9	51.7	n/a
	Cu (ppm)	154	190	308	231	50.0	17.7
	Zn (ppm)	187	209	279	219	33.0	4.6
	Br (ppm)	186	n/d	197	414	5.6	100.0
	Sr (ppm)	725	331	704	1110	n/a	70.2
	Mo (ppm)	n/d	n/d	425	423	100.0	100.0
	Ru (ppm)	420	583	554	524	24.2	n/a
	Pd (ppm)	n/d	459	594	915	100.0	49.8
	W (ppm)	n/d	n/d	n/d	829	n/a	100.0
	V (ppm)	n/d	n/d	111	127	100.0	100.0
Oxides	SiO_2 (ppm)	9100	3060	19,500	1800	53.3	n/a
	Al_2O_3 (ppm)	2050	882	4190	n/d	51.1	n/a
	Fe_2O_3 (ppm)	10,900	4820	24,100	2580	54.8	n/a
	CaO (ppm)	12,400	24,100	22,700	22,300	45.4	n/a
	MgO (ppm)	2200	1910	2760	1550	20.3	n/a
	Na_2O (ppm)	387	1810	967	3850	60.0	53.0
	TiO_2 (ppm)	758	413	1640	230	53.8	n/a
	K_2O (ppm)	7400	33,100	2170	8810	n/a	n/a
	P_2O_5 (ppm)	1170	3270	1300	1300	10.0	n/a
	MnO (ppm)	162	163	880	365	81.6	55.3
	SO_3 (ppm)	3800	7550	9780	4400	61.1	n/a
	V_2O_5 (ppm)	99.8	n/d	249	n/d	59.9	n/a
	SrO (ppm)	379	851	755	789	49.8	n/a
	CuO (ppm)	208	213	378	191	45.0	n/a
	Cr_2O_3 (ppm)	49.5	n/d	265	n/d	81.3	n/a
	ZnO (ppm)	287	218	344	137	16.6	n/a
	NiO (ppm)	88.6	125	239	93.5	62.9	n/a
	MoO_3 (ppm)	n/d	592	603	n/d	100.0	n/a

Table 5 (continued)

		Summer		Winter		Accumulation (%)	
				CVFW-3		CVFW-3	
		Root	Stem	Root	Stem	Root	Stem
Elements	Na (ppm)	1310	284	958	5710	n/a	95.0
	Mg (ppm)	1130	1220	1650	3720	31.5	67.2
	Al (ppm)	408	1100	1630	585	75.0	n/a
	Si (ppm)	1600	4070	6350	3530	74.8	n/a
	P (ppm)	1490	830	1060	4470	n/a	81.4
	S (ppm)	3090	1560	8780	6100	64.8	74.4
	Cl (ppm)	12,700	4470	8550	n/d	n/a	n/a
	K (ppm)	27,400	6250	1550	24,800	n/a	74.8
	Ca (ppm)	17,300	8640	19,400	39,100	10.8	77.9
	Ti (ppm)	194	489	818	220	76.3	n/a
	Cr (ppm)	96.7	116	n/d	n/d	n/a	n/a
	Mn (ppm)	156	96.7	786	473	80.2	79.6
	Fe (ppm)	3450	7820	13,400	3520	74.3	n/a
	Ni (ppm)	112	104	213	n/d	47.4	n/a
	Cu (ppm)	154	190	395	219	61.0	13.2
	Zn (ppm)	187	209	387	361	51.7	42.1
	Br (ppm)	186	n/d	348	620	46.6	100.0
	Sr (ppm)	725	331	691	1660	n/a	80.1
	Mo (ppm)	n/d	n/d	220	398	100.0	100.0
	Ru (ppm)	420	583	500	702	16.0	17.0
	Pd (ppm)	n/d	459	n/d	448	n/a	n/a
	V (ppm)	n/d	n/d	453	82.4	100.0	100.0
Oxides	SiO_2 (ppm)	9100	3060	14,100	7620	35.5	59.8
	Al_2O_3 (ppm)	2050	882	3000	1340	31.7	34.2
	Fe_2O_3 (ppm)	10,900	4820	18,400	4810	40.8	n/a
	CaO (ppm)	12,400	24,100	26,500	53,900	53.2	55.3
	MgO (ppm)	2200	1910	2820	6620	22.0	71.1
	Na_2O (ppm)	387	1810	1190	8450	67.5	78.6
	TiO_2 (ppm)	758	413	1100	268	31.1	n/a
	K_2O (ppm)	7400	33,100	1920	14,200	n/a	n/a
	P_2O_5 (ppm)	1170	3270	2360	10,700	50.4	69.4
	MnO (ppm)	162	163	1030	602	84.3	72.9
	SO_3 (ppm)	3800	7550	21,800	14,900	82.6	49.3
	V_2O_5 (ppm)	99.8	n/d	754	n/d	86.8	n/a
	SrO (ppm)	379	851	776	1780	51.2	52.2
	CuO (ppm)	208	213	503	319	58.6	33.2
	Cr_2O_3 (ppm)	49.5	n/d	n/d	n/d	n/a	n/a
	ZnO (ppm)	287	218	469	480	38.8	54.6
	NiO (ppm)	88.6	125	279	n/d	68.2	n/a
	MoO_3 (ppm)	n/d	592	320	658	100.0	10.0
	WO_3 (ppm)	n/d	n/d	n/d	430	n/a	100.0

Accumulation observed while treating 262 l of wastewater from summer to winter

n/d not detected, *n/a* not applicable

Table 6 Biochemical characteristics of *Dracaena* of CVFWs

Wetland types	Parameters	CVFW-1	CVFW-2	CVFW-3
Summer	Root ash content (%)	0.96	0.96	0.96
	Stem ash content (%)	4.90	4.90	4.90
	Ammonia (mg/l), root	0.82	0.82	0.82
	Ammonia (mg/l), stem	0.82	0.82	0.82
	Phosphate (mg/l), root	0.02	0.02	0.02
	Phosphate (mg/l), stem	0.03	0.03	0.03
	Chlorophyll a (mg/ml)	1.48	1.48	1.48
	Chlorophyll b (mg/ml)	0.95	0.95	0.95
	Total chlorophyll (mg/ml)	2.42	2.42	2.42
Winter	Root ash content (%)	1.73	1.25	1.60
	Stem ash content (%)	5.16	6.97	3.17
	Ammonia (mg/l), root	1.16	1.03	0.90
	Ammonia (mg/l), stem	0.98	1.04	0.98
	Phosphate (mg/l), root	0.05	0.03	0.03
	Phosphate (mg/l), stem	0.06	0.03	0.03
	Chlorophyll a (mg/ml)	2.84	3.29	3.25
	Chlorophyll b (mg/ml)	1.30	1.53	1.35
	Total chlorophyll (mg/ml)	4.01	4.81	4.24

Accumulation observed while treating 262 l of wastewater from summer to winter

Conclusions

In this study, the performance of different "constructed vertical flow wetlands" treating textile dye wastewater (metanil yellow as dye) is investigated for 9 months (covering three seasons). The CVFWs planted with *Dracaena* efficiently removed contaminants like dye, COD, NH_4^+-N, and PO_4^{3-}-P from the wastewater and the removal performance largely depends on meteorological factors. The CVFWs' overall performance is similar for summer and winter, and least in monsoon. Significant dye removal was observed during the study period, maximum in summer (control, 44.3%; CVFW-1, 75.1%; CVFW-2, 76.1%; CVFW-3, 46%), but lesser in winter (control, 45; CVFW-1, 73.1%; CVFW-2, 76.8%; CVFW-3, 42.6%) and the least in monsoon (control, 40.8%; CVFW-1, 63.5%; CVFW-2, 51.6%; CVFW-3, 37.1%), whereas COD removal was observed to be highest in winter (64.4%, CVFW-1; 72.3%, CVFW-2; 62.5%, CVFW-3) followed by summer (61.8%, CVFW-1; 70.5%, CVFW-2; 59.4%, CVFW-3) and monsoon (50.5%, CVFW-1; 57.2%, CVFW-2; 51%, CVFW-3). Nutrients ranged between 52.1 and 64.4% (PO_4^{3-}-P) and 56.6 and 71.6 (NH_4^+-N). CVFW-1 and CVFW-2 performed well, showing no stress on *Dracaena*, whereas CVFW-3 showed lesser performance, which may be due to plant stress resulting from a higher inlet concentration of dye. Dye removal was achieved due to phytoremediation activities and media adsorption. *Dracaena* proved to be efficient in dye removal and other pollutants; however, exceeding dye concentrations (> 50 mg/l) may pose stress. The first-order kinetic model was used to evaluate the decomposition rate constant. Higher K_A values were achieved for dye removal in summer for all CVFWs. Various functional groups were characterized using FTIR from the inlet and outlet water samples of different CVFWs. The pollutant removal efficiency concerning seasons was validated statistically. Dye, COD, and PO_4^{3-}-P removal showed significant differences, highlighting the impact of seasonal variation, whereas NH_4^+-N removal is independent of meteorological factors. The *Dracaena* of the wetlands accumulated various elements and oxides with no stress on its health. Apart from wetland species, there are various robust ornamental plants that can be tested for textile dye wastewater treatment.

Acknowledgements Authors sincerely acknowledge Dr. S. Kannan, Director, CSIR-CSMCRI, Bhavnagar, for providing infrastructural facilities. Meera Keraliya and Mansi Joshi supported the data collection. The authors acknowledge the funding supported by the Science and Engineering Research Board (GOI) [the project grant/file no. SRG/2019/001803] and in-house funding from MLP-0045 project; MM acknowledges the PhD fellowship grant from UGC, Centralized Instrument Facility, for analysis support. The manuscript has been assigned CSIR-CSMCRI-155/2021 registration.

Author contribution Monali Muduli: conceptualization, data curation, and writing—original draft. Meena Choudhary: data curation, review writing, visualization. Soumya Haldar: review and editing. Sanak Ray: conceptualization, visualization, review, supervision, editing, and fund acquisition.

Funding This work was supported by the Start-up Research Grant (the project file no. SRG/2019/001803) of the Science and Engineering Research Board (Govt. of India) and in-house funding from MLP-0045 project.

Data availability Data are available from the authors upon reasonable request.

Declarations

Conflict of interest The authors declare no competing interests.

References

APHA. (2017). *Standard methods for the examination of water and waste water* (23rd ed.). American Public Health Association.

Ali, Y., Shafida, A. H., & Rashid, U. (2018). Biomedical applications of aromatic azo compounds. *Mini Reviews in Medicinal Chemistry, 18*(18), 1548–1558. https://doi.org/10.2174/1389557518666180524113111

Anjaneya, O., Souche, S. Y., Santoshkumar, M., & Karegoudar, T. B. (2011). Decolorization of sulfonated azo dye metanil yellow by newly isolated bacterial strains: Bacillus sp. strain AK1 and Lysinibacillus sp. strain AK2. *Journal of Hazardous Materials, 190*(1–3), 351–358. https://doi.org/10.1016/j.jhazmat.2011.03.044

Benkhaya, S., M'rabet, S., & El Harfi, A. (2020). Classifications, properties, recent synthesis and applications of azo dyes. *Heliyon*, *6*(1). https://doi.org/10.1016/j.heliyon.2020.e03271

Chung, K. T. (2016). Azo dyes and human health: A review. *Journal of Environmental Science and Health - Part C Environmental Carcinogenesis and Ecotoxicology Reviews, 34*(4), 233–261. https://doi.org/10.1080/10590501.2016.1236602

Dadrasnia, A., & Pariatamby, A. (2016). Phyto-enhanced remediation of soil co-contaminated with lead and diesel fuel using biowaste and Dracaena reflexa: A laboratory study. *Waste Management and Research, 34*(3), 246–253. https://doi.org/10.1177/0734242X15621375

Dogdu, G., & Yalcuk, A. (2016). Indigo dyeing wastewater treatment by eco-friendly constructed wetlands using different bedding media. *Desalination and Water Treatment, 57*(32), 15007–15019.

Gajewska, M., Skrzypiec, K., Jó, K., Mucha, Z., Karczmarczyk, A., & Bugajski, P. (2020). Kinetics of pollutants removal in vertical and horizontal flow constructed wetlands in temperate climate. *Science of the Total Environment*. https://doi.org/10.1016/j.scitotenv.2020.137371

Ghosh, D., Singha, P. S., Firdaus, S. B., & Ghosh, S. (2017). Metanil yellow: The toxic food colorant. *Asian Pacific Journal of Health Sciences, 4*(4), 65–66. https://doi.org/10.21276/apjhs.2017.4.4.16

Guerrero-Coronilla, I., Aranda-García, E., & Cristiani-Urbina, E. (2019). Biosorption of metanil yellow dye from aqueous solutions by the entire water hyacinth plant (Eichhornia crassipes) and its vegetative organs. *Environmental Engineering and Management Journal, 18*(8), 1671–1682. https://doi.org/10.30638/eemj.2019.157

Haddaji, D., Ghrabi-Gammar, Z., Hamed, K. B., & Bousselmi, L. (2019). A re-circulating horizontal flow constructed wetland for the treatment of synthetic azo dye at high concentrations. *Environmental Science and Pollution Research, 26*(13), 13489–13501.

Hussein, A., & Scholz, M. (2018). Treatment of artificial wastewater containing two azo textile dyes by vertical-flow constructed wetlands. *Environmental Science and Pollution Research, 25*(7), 6870–6889. https://doi.org/10.1007/s11356-017-0992-0

Indian Meteorological Department. (2020). Retrieved 2 March 2020 to 24 November 2020, from https://mausam.imd.gov.in/

Kourani, K., Kapoor, N., Badiye, A., & Shukla, R. K. (2020). Detection of synthetic food color "metanil yellow" in sweets: A systematic approach. *Journal of Planar Chromatography - Modern TLC, 33*(4), 413–418. https://doi.org/10.1007/s00764-020-00046-9

Ladwani, K. D., Ladwani, K. D., Ramteke, D. S., & Deo, S. (2016). Detection and identification of organic compounds in wastewater of final effluent treatment plant by FTIR and GC-MS. *Journal of Advanced Chemical Sciences, 2*(2), 246-247.

Lee, J., Lee, S., & Yu, S. (2016). Relationships between water quality parameters in rivers and lakes: BOD 5, COD, NBOPs, and TOC. *Environmental Monitoring and Assessment*. https://doi.org/10.1007/s10661-016-5251-1

Li, Y., Yang, H. Y., Shen, J. Y., Mu, Y., & Yu, H. Q. (2016). Enhancement of azo dye decolourization in a MFC-MEC coupled system. *Bioresource Technology, 202*, 93–100. https://doi.org/10.1016/j.biortech.2015.11.079

Matyszczak, G., Sędkowska, A., & Kuś, S. (2020). Comparative degradation of metanil yellow in the electro-Fenton process with different catalysts: A simplified kinetic model study. *Dyes and Pigments*, *174*(July). https://doi.org/10.1016/j.dyepig.2019.108076

Mohanty, A., Ray, S., Yadav, A. K., & Chaudhury, G. R. (2015). NH_3 and COD removal from wastewater using biological process: Kinetics with optimization studies. *Desalination and Water Treatment, 53*(3), 658–670.

Muduli, M., Sonpal, V., Ray, S., & Haldar, S. (2022). In-depth performance study of an innovative decentralized multistage constructed wetland system treating real institutional wastewater. *Environmental Research, 210*, 112896. https://doi.org/10.1016/j.envres.2022.112896

Nandakumar, S., Pipil, H., Ray, S., & Haritash, A. K. (2019). Removal of phosphorous and nitrogen from wastewater in Brachiaria-based constructed wetland. *Chemosphere, 233*, 216–222.

Oon, Y. L., Ong, S. A., Ho, L. N., Wong, Y. S., Dahalan, F. A., Oon, Y. S., et al. (2020). Constructed wetland–microbial fuel cell for azo dyes degradation and energy recovery: Influence of molecular structure, kinetics, mechanisms and degradation pathways. *Science of the Total Environment, 720*, 137370. https://doi.org/10.1016/j.scitotenv.2020.137370

Ramadhani, P., Chaidir, Z., Zilfa, Z., Tomi, Z. B., Rahmiarti, D., & Zein, R. (2020). Shrimp shell (Metapenaeus monoceros) waste as a low-cost adsorbent for metanil yellow dye removal in aqueous solution. *Desalination and Water Treatment, 197*, 413–423. https://doi.org/10.5004/dwt.2020.25963

Ray, S., Mohanty, A., Mohanty, S. S., Mishra, S., & Chaudhury, G. R. (2014a). Optimization of biological elimination of ammonia and COD from waste water using response surface methodology. *Clean-Soil, Air, Water, 42*(12), 1744–1750.

Ray, S., Mohanty, A., Mohanty, S. S., Mishra, S., & Chaudhury, G. R. (2014b). Removal of nitrate and COD from wastewater using denitrification process: Kinetic, optimization, and statistical studies. *Clean Technologies and Environmental Policy, 16*(2), 291–301.

Ray, S., Scholz, M., & Haritash, A. K. (2019). Kinetics of carbon and nitrogen assimilation by heterotrophic microorganisms during wastewater treatment. *Environmental Monitoring and Assessment, 191*(7), 451.

Tee, H. C., Lim, P. E., Seng, C. E., Mohd Nawi, M. A., & Adnan, R. (2015). Enhancement of azo dye acid orange 7 removal in newly developed horizontal subsurface-flow constructed wetland. *Journal of Environmental Management, 147*, 349–355. https://doi.org/10.1016/j.jenvman.2014.09.025

Yaseen, D. A., & Scholz, M. (2017). Comparison of experimental ponds for the treatment of dye wastewater under controlled and semi-natural conditions. *Environmental Science and Pollution Research, 24*(19), 16031–16040. https://doi.org/10.1007/s11356-017-9245-5

Yin, H., Yan, X., & Gu, X. (2017). Evaluation of thermally-modified calcium-rich attapulgite as a low-cost substrate for rapid phosphorus removal in constructed wetlands. *Water Research, 115*, 329–338. https://doi.org/10.1016/j.watres.2017.03.014

Zou, H., & Wang, Y. (2017). Azo dyes wastewater treatment and simultaneous electricity generation in a novel process of electrolysis cell combined with microbial fuel cell. *Bioresource Technology, 235*, 167–175. https://doi.org/10.1016/j.biortech.2017.03.093